BJR https://doi.org/10.1259/bjr.20220384

Received: 07 April 2022 | Accepted: 03 March 2023 | Published online: 25 April 2023

Cite this article as:
Pang Y, Kosmin M, Li Z, Deng X, Li Z, Li X, et al. Isotoxic dose escalated radiotherapy for glioblastoma based on diffusion-weighted MRI and tumor control probability—an in-silico study. *Br J Radiol* (2023) 10.1259/bjr.20220384.

FULL PAPER

Isotoxic dose escalated radiotherapy for glioblastoma based on diffusion-weighted MRI and tumor control probability—an in-silico study

[1]YARU PANG, PhD, [2,3]MICHAEL KOSMIN, MD, [4]ZHUANGLING LI, MD, [4]XIAONIAN DENG, MD, [4]ZIHUANG LI, MD, [4]XIANMING LI, MD, [1]YING ZHANG, PhD, [1]GARY ROYLE, PhD and [1,5]SPYROS MANOLOPOULOS, PhD

[1]Department of Medical Physics and Biomedical Engineering, University College London, Gower Street, London, United Kingdom
[2]Neuro-Oncology Team, Department of Oncology, University College London Hospital NHS Foundation Trust, 250 Euston Road, London, United Kingdom
[3]National Institute for Health Research University College London Hospitals (UCLH) Biomedical Research Centre, London, United Kingdom
[4]Department of Radiation Oncology, Shenzhen People's Hospital, Shenzhen, China
[5]Northern Centre for Cancer Care, Newcastle upon Tyne Hospitals NHS Foundation Trust, Carlise, United Kingdom

Address correspondence to: Yaru Pang
E-mail: *yaru.pang.17@ucl.ac.uk*

Objectives: Glioblastoma (GBM) is the most common malignant primary brain tumor with local recurrence after radiotherapy (RT), the most common mode of failure. Standard RT practice applies the prescription dose uniformly across tumor volume disregarding radiological tumor heterogeneity. We present a novel strategy using diffusion-weighted (DW-) MRI to calculate the cellular density within the gross tumor volume (GTV) in order to facilitate dose escalation to a biological target volume (BTV) to improve tumor control probability (TCP).

Methods: The pre-treatment apparent diffusion coefficient (ADC) maps derived from DW-MRI of ten GBM patients treated with radical chemoradiotherapy were used to calculate the local cellular density based on published data. Then, a TCP model was used to calculate TCP maps from the derived cell density values. The dose was escalated using a simultaneous integrated boost (SIB) to the BTV, defined as the voxels for which the expected pre-boost TCP was in the lowest quartile of the TCP range for each patient. The SIB dose was chosen so that the TCP in the BTV increased to match the average TCP of the whole tumor.

Results: By applying a SIB of between 3.60 Gy and 16.80 Gy isotoxically to the BTV, the cohort's calculated TCP increased by a mean of 8.44% (ranging from 7.19 to 16.84%). The radiation dose to organ at risk is still under their tolerance.

Conclusions: Our findings indicate that TCPs of GBM patients could be increased by escalating radiation doses to intratumoral locations guided by the patient's biology (*i.e.,* cellularity), moreover offering the possibility for personalized RT GBM treatments.

Advances in knowledge: A personalized and voxel level SIB radiotherapy method for GBM is proposed using DW-MRI, which can increase the tumor control probability and maintain organ at risk dose constraints.

INTRODUCTION

Glioblastoma Multiforme (GBM), a WHO Grade four glioma, is the most common malignant primary brain tumor.[1] The standard treatment for patients younger than 70 years old and Karnofsky Performance Status (KPS) more than 70 is 60 Gy radiotherapy delivered in 30 fractions (2 Gy per fraction) with concurrent and adjuvant temozolomide chemotherapy. For patients older than 70 years old and/or KPS less than 70, treatment to 40.05 Gy in 15 fractions with concurrent and adjuvant temozolomide chemotherapy can be considered.[2] However, long term control is hard to achieve with median survival time of 15–18 months and 2-year survival rate of 26–33%.[3,4] Most recurrences after radiotherapy occur inside the irradiated area, at a rate from 58 to 92%[5–9] suggesting that the prescribed radiation dose is not sufficient for control, therefore increasing the radiation dose should reduce local recurrences. However, clinical trials where the dose was escalated uniformly across the tumor have shown an increase in toxicity because of the associated increased dose to the surrounding healthy tissues and organs at risk (OARs).[10,11] An alternative strategy is to identify intratumoural areas with a higher risk

of progression to escalate the dose isotoxically, i.e., respecting the same dose-volume constraints for OARs as per the standard treatment (of 60 Gy in 30 fractions). This is called isotoxic dose escalation, achievable by "dose painting" as proposed by Clifton Ling.[12]

Over the last 20 years, many clinical trials have been conducted using functional imaging (*e.g.,* PET or MRI) to identify radioresistant areas within various tumors.[13–18] Compared with conventional anatomical imaging modalities such as CT and T1/T_2 weighted MRI, functional imaging can provide additional information on tumor heterogeneity by providing information on organ physiological function.[17] In turn, this data could facilitate the planning and delivery of radiotherapy.[18] For GBM, some studies employed functional imaging techniques, such as positron emission topography (PET) and magnetic resonance spectrum imaging (MRSI) to define the high-risk areas.[19–24] In addition, since tumor cell density is considered as an important factor that determines the treatment outcome,[25–28] use of diffusion-weighted magnetic resonance imaging (DW-MRI) allows us to measure the *in vivo* density of cells inside the body.[29,30]

Standard radiobiological theory dictates that the radiation dose should increase in proportion with the number of tumor cells in order to increase the probability to stop a tumour's growth or even eradicate it.[31,32] DW-MRI-based dose painting can identify area with insufficient dose to achieve control and then direct a boost of dose accordingly. DW-MRI is converted into apparent diffusion coefficient (ADC) maps, which are inversely correlated with tumor cell density.[33–42]

Since ADC values have been demonstrated as a significant association with overall survival,[43,44] in our study, we use ADC maps to calculate tumor cell density and derive voxelised (3D) cell distributions. A personalized biological model is employed to calculate the voxel-level tumor control probability (TCP) that corresponds to the planned dose distribution for each patient treatment. This in turn is used to change the radiotherapy plan, by following a dose painting method to escalate the dose focally at specific intratumoural areas, which showed a higher disease burden, in order to increase the TCP.

METHODS

In our work, pre-treatment ADC maps were derived from DW-MRI of ten GBM patients treated with radical chemoradiotherapy (60 Gy in 30 fractions) and are used to calculate the cell density (per voxel) in their gross tumor volumes (GTVs) using an empirical formula, shown below.[42] Since GTVs are defined on the radiotherapy planning CT, as per routine clinical practice, to correspond to the macroscopically manifested malignancy based on CT and MRI (T1, FLAIR), a rigid registration between ADC maps and the planning CT images was performed to register the GTV structure on the ADC images. A Poissonian linear quadratic (LQ) TCP model (with radiosensitivity parameters of $\alpha = 0.12$ Gy^{-1}, $\beta = 0.015$ Gy^{-2}[45]) was used to calculate the three-dimensional (voxelated) TCP maps that correspond to the cell density distributions within the GTVs, as determined from the corresponding ADC maps. Those GTV regions with TCPs in the lowest quartile of the TCP range for each patient were designated as the GTV subvolumes with a higher risk for recurrence after radiotherapy and labeled the biological target volume (BTV). The BTV dose was escalated using a simultaneous integrated boost (SIB) aiming to increase the TCP within the BTV to the median TCP value for each case in turn. The SIB dose itself was defined as that required to achieve this objective for each case individually. Finally, radiotherapy treatments were simulated using the clinical plans as a baseline and incorporating the corresponding BTVs and the associated SIB dose derived for each patient case. Dose constraints to the surrounding organs at risk (OARs) were not changed from the baseline standard clinical plans, and personalized SIB plans were created accordingly.

Dataset

We studied 10 patients with GBM who were treated between 2018 to 2019 with standard radical chemoradiotherapy of 60 Gy in 30 fractions with concomitant and adjuvant temozolomide. Our study was approved by the local ethics committee and written informed consent was obtained by the patients before their treatment. All enrolled patients had CT and anatomical MR imaging acquired before radiotherapy and used for treatment planning purposes. After segmenting the tumor-related target volumes and healthy organs at risk according to standard clinical protocols, volumetric-modulated arc therapy (VMAT) treatments were planned using the Eclipse 13.6 system to be delivered by a True Beam linear accelerator (Varian Medical Systems, Palo Alto, California). All the patients received prior surgery and the GTV included resection cavities in all cases. The target delineation was based on European Society Radiation Oncology (EORTC) protocol. Doses in the target volume were prescribed by 60 Gy in 30 fractions. The GTV was defined from the planning CT data and postoperative images from MRI fusion, and was shown as enhancing tumor and resection cavity on contrast-enhanced T_1 weighted MRI. The clinical target volume (CTV) was GTV + 2 cm. The volume was trimmed at the bony circumference, tentorium and midline, unless there was a clear route for tumor spread such as the corpus callosum. The planning target volume (PTV) was CTV + 0.3 cm. DW-MRI was acquired on a 3T scanner (Magnetom Verio, Siemens Medical Systems, Erlangen, Germany) with an echo-planar (EPI) sequence using b-values of 400, 800 and 1000 s/mm2 as the average diffusion values along three orthogonal axes, repetition times (TR) between 4600 to 13300 s, echo time (TE) = 72–95 s, flip angle = 90, GRAPPA accelerator factor = 2 and EPI factor of 132. ADC maps were computed using all b-values, with a voxel size of 1.2 × 1.2 × 6.5 mm^3. For the enrolled patients, quantities summarizing dose distributions in the GTV, CTV and PTV volumes are given in Supplementary data 1.

Cell density map

The DWI-derived ADC maps were related to the cell density of the corresponding volume element (voxel). To achieve this, ADC maps were registered to the planning CT scans using rigid registration to anatomical landmarks, *e.g.*, the skull. The voxel size of each CT image is 0.926 × 0.926 × 3.000 mm^3. The matrix size for the patient data was 192 × 192 × 19 voxels for the ADC and 512 × 512 × 99 for the CT images respectively. The NiftyReg software[46]

Figure 1. Cell density and the corresponding ADC values derived by Eidel *el al*.[42] ; the line represents a linear fit performed herein using equation (1). Pearson's r = −0.40; Spearman's R_s = −0.48, both with p-values less than 0.01.

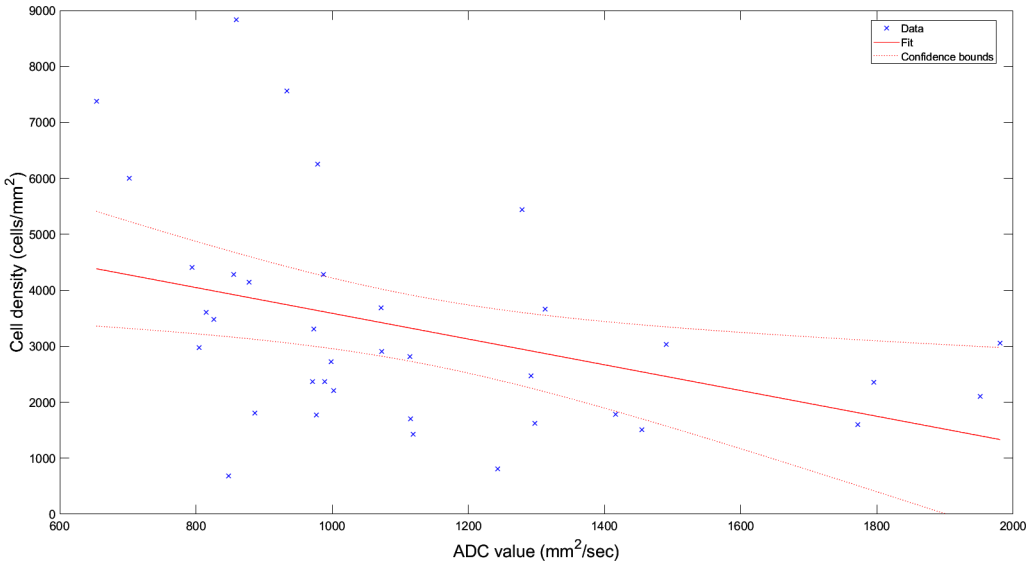

was used to register ADC maps on CT images by resampling ADC voxels using trilinear interpolation in order to match with the CT grid, leading to a 512 × 512 × 99 cell density map. On each CT-ADC registered image plane, cell densities are calculated. Several studies indicate that there is an inverse correlation between ADC and cell density.[38–42,45,47–50] Eidel et al[42] quantified the relationship between ADC and cell density for GBM, as is shown in Figure 1. These data can be fitted linearly using the following formula:

$$\text{cell density}(\rho) = -2.3 \times ADC + 5889.6, \quad (1)$$

where the coefficients are derived by the best fit. Equation (1) was also used to calculate the cell density from the ADC values for our patient data. We considered ADC values from 460 to 1660 mm^2/s to indicate malignancy as reported by others.[47–50]

TCP map

A linear-quadratic (LQ) TCP model defined in Equation (2) is used to calculate voxelated TCP_i values, where N_i is the number of tumor cells per voxel; D_i is the voxelated total treatment dose; d_i is the voxelated dose per fraction; n is the number of fractions; α and β are tissue radiobiological parameters chosen as $\alpha = 0.12\ Gy^{-1}$, $\beta = 0.015\ Gy^{-2}$[51] ; ρ_i is the cell density in the area (A) of $0.926 \times 0.926\ mm^2$ calculated in Section 2.2.

$$\begin{aligned} \text{TCPi} &= exp\left(-N_i\, exp\left(-\left(\alpha + \beta d_i\right) D_i\right)\right) \\ &= exp\left(-\rho_i A\, exp\left(-\left(\alpha + \beta D_i/n\right) D_i\right)\right) \end{aligned} \quad (2)$$

The above equation can be used to calculate the TCP_i for a given cell density at each pixel (ρ_i), with the latter derived from the ADC maps. Repeating for all pixels in the ADC image produces a volumetric (3D) TCP map for the available data.

Biological tumor volume (BTV) and simultaneous integrated boost (SIB)

The aforementioned TCP map is used to define biological target volume (BTV), where the dose will be escalated by means of a simultaneous integrated boost (SIB), that is increasing the dose per fraction whilst maintaining the same number of fractions (*i.e.,* 30). We calculate the voxelated TCP values in the GTV, and define the BTV as the volume in which the TCP values are in the lowest quartile of the calculated TCP range for that patient.

Each patient's SIB dose is calculated such that the minimum TCP in the BTV is increased to match the median TCP value of the whole tumor. The SIB dose is achieved by finding the root of quadratic equation below, and the corresponding derivation is presented in the supplementary data 2.

$$\left(\alpha + \beta\frac{D_{SIB}}{n}\right) D_{SIB} = \log\left(\frac{\log\left(TCP_{high}\right)}{\log\left(TCP_{low}\right)}\right) - \left(\alpha + \beta\frac{D}{n}\right) D \quad (3)$$

where TCP_{low} is the minimum TCP of the BTV; TCP_{high} is the median TCP of the whole GTV; D is the original prescription dose, *i.e.,* 60 Gy; D_SIB is the SIB dose prescribed to the BTV; n is the number of treatment fractions. Taking patient one as an example, the original prescription dose is 60 Gy in 30 fractions. TCP_{low} is 70.18% in the BTV, and TCP_{high} is 80.76% in the GTV, respectively. Use of Equation (3) allows us to calculate SIB dose to be 66.6 Gy in 30 fractions.

SIB isotoxic dose escalation

The SIB isotoxic dose escalation plans were performed on the Varian Eclipse dose planning system with the VMAT technique, which is used for the original clinical plans. Then, BTV was generated in the TPS for each patient following our proposed method in Section 2.4. The radiation dose to the area of PTV

Figure 2. The flow charts of the methods applied to obtain escalated SIB isotoxic dose.

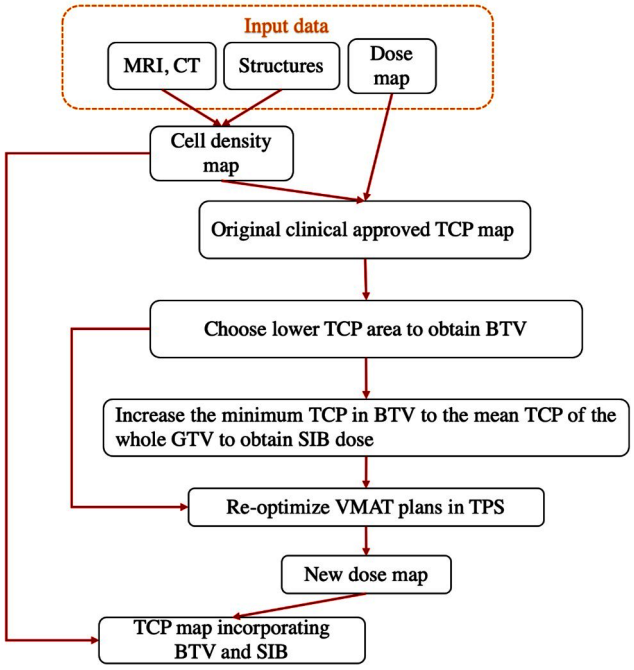

excluding BTV was still 60 Gy in 30 fractions. In BTV, the same number of fractions are used, and radiation was delivered as a simultaneous integrated boost with the personalized SIB dose on a case-by-case basis. Mirroring the original clinical plans, the dose-volume optimization objectives for the target and OAR constraints are given in Supplementary data 2. To confirm the feasibility of SIB isotoxic dose escalation plans, we evaluated whether the dose in BTV and PTV achieve the requested dose levels, and whether the dose in OARs stays within their tolerance when changing the dose prescription. Once the SIB isotoxic dose escalation plans have been approved by an oncologist, a new dose distribution map was generated. Combined with the cell density map mentioned in Section 2.2, a new TCP map was generated. The SIB isotoxic dose escalation plans were compared to the clinical delivered plans with respect to TCP maps. We can then demonstrate how TCP growth behaves in TPS. Figure 2 shows the step-by-step operation of the proposed SIB isotoxic dose escalation.

RESULTS

For our patient cohort, the ADC values inside the GTVs ranged from 470 to 1660 mm^2/s. Figure 3 shows the BTV, and SIB dose calculated for the patient referred in Section 2.4 as an example case. Figure 3(a) shows a "slice" (axial-plane distribution) of the patient's ADC map with the corresponding GTV (red line) outlined on the CT images and transferred as a result of the ADC-CT image fusion. Figure 3(b) shows the corresponding cell density map, calculated using equation (1), as described in Section 2.2. The red and blue colored areas correspond to GTV regions with the higher and lower cell densities, respectively. Using equation (2) in Section 2.3, the corresponding TCP map can be derived, which is shown in Figure 3(c). For this patient, the TCP ranges from 0.7018 to 0.9258 with a median of 0.8076.

Figure 3. Stepwise analysis to deduce BTV and SIB dose on the same axial plane of the example patient: (a) ADC image and outlined GTV, (b) the calculated cell density, (c) the TCP that corresponds to the clinical dose distribution (60 Gy in 30 fractions), (d) the derived BTV, (e)boosted dose distribution and its corresponding TCP map (f).

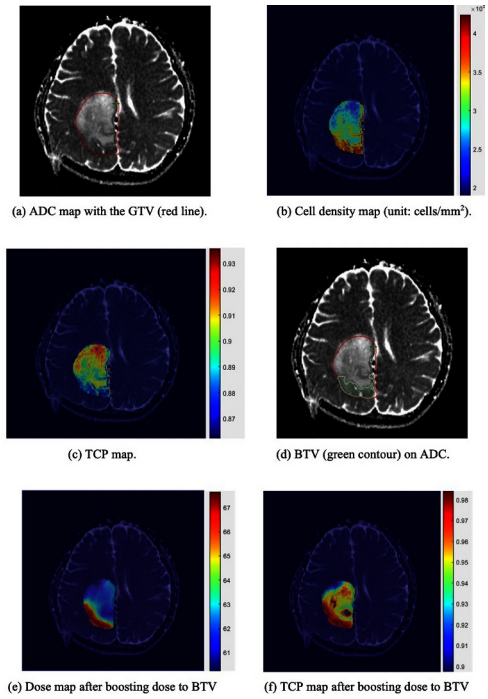

Areas with TCP values between 0.7018 and 0.7578 correspond to the lowest quartile, and were used to define the BTV, as shown in Figure 3(d), where ADC values range from 478 to 783 mm^2/s. Given the calculated TCP values, the SIB dose (DSIB) was calculated as 66.6 Gy using Equation (3). The SIB isotoxic dose escalation plans were then performed on the Varian Eclipse dose planning system with the VMAT technique. The radiation dose to the area of PTV excluding BTV was still 60 Gy in 30 fractions. After boosting the SIB dose to BTV, the dose map of this layer was shown in Figure 3 (e) for this patient. The TCP map of the same layer after SIB isotoxic dose escalation planning was shown in Figure 3 (f).

The histogram distribution with the TCP values from all voxels in the clinical plan (prescribed dose 60 Gy, no SIB), for this patient is shown in Figure 4 (blue bars). This is produced by the accumulation of maps as per Figure 3(c), from all "slices" of the complete 3D image dataset. The TCP values that correspond to the SIB plan are shown in Figure 4, orange bars. Comparing the corresponding TCP values of the clinical plan (no SIB) and the SIB plan, the latter TCP has increased from values ranging between 70.18 and 92.58% to between 87.92 and 99.20% respectively (Table 1, patient 1). Although the treatment objective is to increase doses only within BTV, there is an unavoidable dose increase to the adjacent voxels, because of a finite dose gradient governed by the laws of physics. Therefore, the dose is increased in larger area than the BTV, thereby elevating the TCP in a wider area within the gross tumor volume.

Figure 4. TCP distributions with and without our method, where x-axis represents the TCP levels and y-axis represents the proportion of each TCP level. Blue bars represent the TCP values from all voxels in the clinical plan for this patient, while orange bars represent TCP values that corresponds to the SIB escalated dose to the BTV.

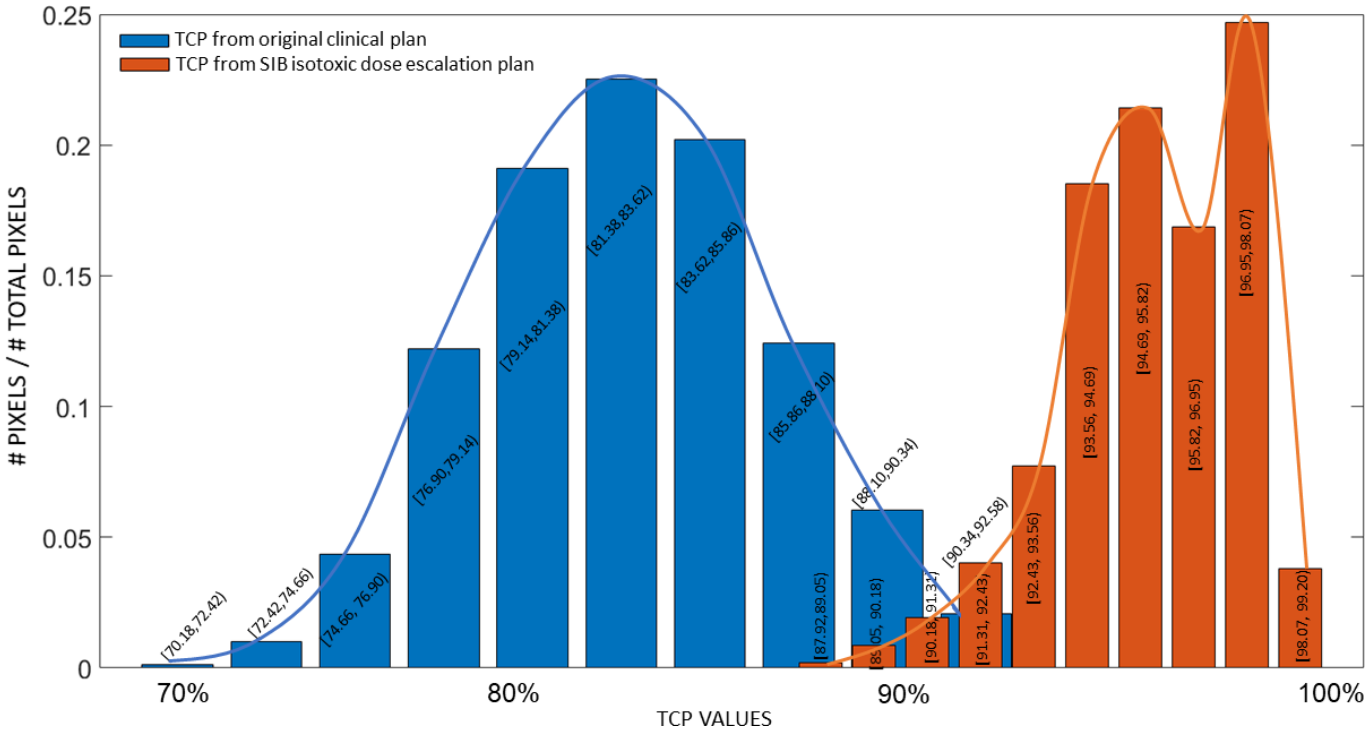

The corresponding results for the ten patients in our cohort are shown in Table 1, which also shows the ADC values in GTV and BTV, number of tumor cells, boost doses (DSIB-D) and TCP increases in clinical dose distributions. Considering the confidence interval in the relationship between ADC values and cell densities, as shown in Figure 4, the corresponding SIB doses and TCP ranges have been calculated and presented in Table 1. The maximum total TCP increase achieved is 16.84%. The volume of BTVs for each patient was shown in Table 2. Since BTVs represent high cell density area, we further investigate how much of the relapsed volume overlaps with BTVs. In Table 2, Patient #1 relapsed three years after radiotherapy, where this patient's BTV is 17.31 cm^3, and the recurrence area within the BTV is 10.80 cm^3, accounting for 62.39% of the BTV. As for the other nine

Table 1. Results of proposed method for 10 GBM patients

	ADC in GTV (mm^2/sec)							TCP increase (%)
Patient	min	max	mean	std	Number of tumor cells	ADC in BTV (mm^2/sec)	Boosted dose (Gy)	*TCP without BTV* V.S. *TCP incorporating BTV and SIB dose*
1	478	1660	1211.05	236.20	$2.88E+10$	478–783	6.60 [6.23, 6.89]	9.42 [6.36, 11.96]
2	624	1656	1201	268.93	$1.23E+09$	624–885	3.60 [3.25, 3.67]	7.19 [6.52, 9.61]
3	493	1660	1011	265.39	$5.01E+09$	493–794	6.60 [6.21, 6.68]	7.90 [7.12, 10.58]
4	475	1660	1021.8	266.66	$1.30E+10$	475–689	7.19 [6.83, 7.43]	8.56 [7.95, 11.90]
5	472	1660	1150.8	248.81	$1.39E+10$	472–798	3.90 [3.40, 4.13]	7.57 [7.25, 11.08]
6	495	1660	1096.8	294.85	$1.31E+10$	495–813	16.80 [16.28, 18.41]	8.90 [7.98, 11.76]
7	482	1657	856.61	166.92	$2.98E+10$	482–785	8.02 [7.78, 8.40]	13.64 [12.65, 19.46]
8	512	1657	1075	222.99	$7.88E+09$	512–806	13.20 [12.97, 13.62]	7.24 [6.96, 10.50]
9	488	1660	1106.6	247.29	$1.07E+10$	488–808	8.70 [8.31, 8.98]	8.07 [7.63, 11.39]
10	470	1660	1061.7	299.18	$2.26E+10$	471–797	10.20 [9.88, 10.53]	16.84 [15.46, 23.36]

Table 2. The volume of BTVs for each patient

Patient	GTV volume(cm^3)	BTV volume(cm^3)
1	106.3	17.31
2	5.7	0.4
3	16.7	3.63
4	82.1	6.27
5	57.6	1.82
6	82.0	20.50
7	82.9	5.30
8	42.56	8.14
9	45.48	2.82
10	95.25	8.24

patients, outcome data are not available due to the patients being treated at a centralized oncology center, with their ongoing care managed by different teams.

Table 3 shows the comprehensive OAR dose-volume statistics for the original clinical plan (labelled "old") and the one with the SIB isotoxic dose escalation plan (labelled "new") for each patient. The radiation dose to OARs did not exceed their tolerances, which are shown underneath each OAR. This demonstrates that our SIB doses assigned in BTV, should keep the toxicity to the surrounding OARs to levels that are deemed acceptable as per routine clinical practice. For some patients, the doses to OARs in the SIB plans are less than those in the original clinical plans due to specific treatment planning optimizations.

DISCUSSION

Our study used ADC values derived from functional imaging DW-MRI as imaging biomarkers, following the observation that lower ADC values indicate higher cell density.[42] We then built an MRI-based TCP model to develop a personalized ADC-based dose painting for GBM. Since higher doses increase tumor cell kill,[31,32] through escalating the dose to personalized levels by means of a SIB to each patient's BTV, we achieved an up-to 16.84% increase of TCP for our patient cohort, without exceeding the dose tolerance of the OARs. Our method increases doses by 6–28% among our patient cohort, in the area within the tumor with the highest cell density.

Other ADC-guided dose painting studies have been conducted for patients with head and neck or prostate cancer.[51,54–56] Gronlund et al[18] proposed an optimization method for the dose painting, where the mean dose after optimization equals the original prescription dose. This redistributes the dose over the entire tumor, resulting in some areas getting a lower dose than what was originally prescribed,[27] resulting in unfavorable outcomes.

To our knowledge, the only approach using ADC-based dose painting for GBM was published by Orlanri et al..[57] However, their study was designed for recurrent GBM, not for newly diagnosed GBM.[57] Their optimized prescription dose was only related to ADC values, however, the number of tumor cells was not considered. In addition, even though many dose painting studies used logistic TCP models, the tumor cells repair related to the dose-response of cell survival is not considered. Since the number of tumor cells and tumor cells repair (*i.e.,* radiation sensitivity factors α and β) have been incorporated in linear-quadratic (LQ) TCP models,[45,58] a generalized version of the LQ TCP model was used, with parameters (α and β) corresponding to GBM in this study for planning RT in a personalized way to improve treatment outcomes. We wanted to develop a formalism that could be used widely and transferable to calculations using different TCP parameters for specific types of tumors, different formulations (*e.g.*, including cell repopulation), or even different TCP models corresponding to a different endpoint (*e.g.*, time to progression). Moreover, our approach, albeit utilizing a generalized TCP model, allows for personalized RT, since the level of dose escalation differs between patients.

In contrast to what has been done in other studies, our study combined ADC maps with the voxelated TCP map to achieve the personalized SIB isotoxic dose escalation for GBM. DW-MRI is a well-established method to characterize oncological lesions in terms of cellular density by means of ADC. The inclusion of this information at the cellular level in TCP models may increase the accuracy of tumor control prediction, paving the way towards personalized and optimized treatments.

Since the original prescription dose was the same for each patient, the only factor contributing to TCP is the number of tumor cells. Therefore, for patients with a higher number of tumor cells, a higher TCP increase is expected. This means that our proposed method would benefit more the patients with the higher disease burden and thus worse original prognosis.

We remark that any uncertainties in the underlying DW-MRI images and the corresponding ADC values, could affect the derived cell density,[42] which in turn will affect the values of TCP. However, this should not affect the main findings of our method, because we use only relative TCP values, moreover with the lowest quartile of the TCP range to define the BTV, where the dose would be escalated to increase the overall TCP.

When performing the treatment plan in TPS, there exists a wider dose-increased area than BTV because of finite dose gradients governed by the laws of physics. The doses to OARs could be increased inevitably even although they are still at tolerable levels in our work. It is worth noting that several studies disclosed limitations when performing dose-escalated RT in GBM. Nakagawa et al[10] and Fitzek et al[11] conducted clinical trials and their results showed that escalated RT did not improve survival for GBM patients. This was because toxicity was increased due to higher doses to OARs and normal tissues, caused by escalating the dose to the whole tumor. Our proposed method, instead, increased the dose to a high-risk area within the tumor, whilst keeping the doses to OARs and normal tissues within the established tolerance levels as per the routine clinical practice. Laprie et al[23,59] prescribed a boosted dose of 72 Gy to the MR

Table 3. Dose of the OARs for the ten patients, expressed n terms of maximum doses in optic nerves, optic chiasm, eyes and lens and D0.1cc in brainstem. The dose tolerance indicated by the QUANTEC or RTOG 0825 protocols for those organs are also presented.[52,53]

OARs	Brain Stem		Optic Nerve Left		Optic Nerve Right		Optic Chiasm		Eye globe Left		Eye globe Right		Lens Left		Lens Right	
OARs tolerance	D0.1cc≤55Gy		Dmax≤50Gy		Dmax≤50Gy		Dmax≤55Gy		Dmax≤45Gy		Dmax≤45Gy		Dmax≤10Gy		Dmax≤10Gy	
	old[a]	new[a]	old	new	old	new	old	new	old	new	old	new	old	new	old	new
Patient 1	53.44	53.19	12.23	14.64	14.72	16.63	19.31	21.30	9.70	14.01	15.16	16.72	7.27	7.18	7.17	7.18
Patient 2	24.74	5.12	3.33	2.62	2.78	1.43	5.72	2.78	16.04	6.44	14.42	4.93	3.04	1.22	3.69	1.12
Patient 3	7.28	6.89	2.31	2.43	2.70	2.76	3.47	3.60	1.96	2.06	2.05	2.60	1.07	0.95	1.13	0.99
Patient 4	57.00	51.66	21.43	23.91	52.63	45.93	54.37	49.10	13.17	13.83	25.58	28.45	6.25	4.05	6.84	6.79
Patient 5	56.00[b]	54.82	46.93	34.31	33.67	32.93	52.61	53.98	23.50	23.10	21.04	20.56	8.33	5.87	8.21	6.01
Patient 6	53.85	50.30	11.67	12.26	33.67	14.33	40.32	33.98	54.48	44.42	60.91[b]	44.03	7.92	8.31	7.10	7.13
Patient 7	53.92	51.95	31.06	29.36	22.56	25.74	46.07	49.88	18.95	17.01	16.58	24.30	6.85	4.02	6.78	7.09
Patient 8	6.12	7.10	2.45	2.35	2.14	2.16	4.38	4.20	5.68	5.26	2.95	2.11	1.66	1.36	1.51	1.19
Patient 9	54.06	51.73	28.38	28.35	52.85	48.46	53.46	54.82	13.97	24.15	24.63	29.46	7.26	4.52	7.65	9.65
Patient 10	3.48	4.52	1.30	1.83	1.28	1.57	1.91	2.67	1.21	1.78	1.11	1.30	0.69	0.85	0.73	0.75

[a]old: standard clinical plan; new: SIB plan utilizing the proposed method.

[b]In the original clinical plans, radiation doses to the brainstem of patient 5 and the eye globes of patient 6 exceeded their tolerance, which would not be clinically acceptable. However, in our proposed SIB isotoxic dose escalation plans, all OARs are within their tolerance.

spectroscopic imaging metabolic volumes of CHO/NAA > 2 and contrast-enhancing lesions or resection cavities. Their results showed that the overall survival was not increased compared with the Stupp protocol.[2] Piroth et al escalated the total dose to 72 Gy which did not lead to a survival benefit.[20] They suggested that future studies should be directed to a down-sized PTV and further escalated dose levels to the tumor.[20] To our best knowledge, previous dose-escalated studies used the same boosted dose for the whole patient cohort, while one of our novelties in the proposed method was to increase the dose individually. Singh et al[60] conducted a meta-analysis of 22 prospective trials and concluded that there was no statistical difference ($p > 0.05$) with the addition of TMZ between radiation therapy with or without dose escalation. However, for RT plus TMZ, the estimated overall survival (OS) of dose-escalated treatments is higher than those using standard doses, and for RT without TMZ, dose escalation leads to a significant improvement in progression-free survival (PFS) and OS compared to conventional irradiation. By reviewing the collected patient datasets from this article, wide 95% confidence intervals exist, which indicates large dispersion of the sample data. In addition, some standard-dose RT studies in Singh et al.'s meta-analysis utilized other methods (*e.g.*, increasing the cycles of chemotherapy) to increase the OS and PFS, even although the prescription doses were not escalated.

Many studies also presented some benefits from dose-escalated RT in GBM. Nakagawa et al[10] showed a significant decrease in the rate of local failure, even although increasing the dose did not improve the treatment outcome. With the development of RT techniques, doses can be escalated with iso-toxicity. Iuchi et al conducted a Phase II clinical trial of hypofractionated high-dose IMRT and concluded that the survival of GBM patients has been prolonged.[61] Tsien et al delivered 66 Gy-81Gy to GTV + 0.5 cm, resulting in favourable median OS.[21] In particular, recent studies suggested that for patients who are MGMT unmethylated[62] and cannot tolerate concurrent and adjuvant TMZ,[60] dose-escalated RT can improve OS and PFS.

Another limitation of this study is that even although we considered the uncertainties of the ADC values and cell density, the real link between cell density and radio-resistance is likely to be more complex than implied by this study, which needs to be further improved in the future.

It is foreseeable that the proposed method can be used for the design of clinical trials and our planning study is the first step to that end. To increase the statistical power of our study, we plan to continue enrolling more recurrence GBM patients with DW-MRI, to investigate the correlation of progression regions with pre-radiotherapy ADC values. Given the aforementioned limitations and advantages of dose-escalated RT studies, appropriate patient selection needs to be warranted when using our proposed method to design clinical trials, such as treating TMZ intolerant patients.

In this work, the dose was escalated uniformly to the high risk volume, *i.e.*, BTV, following the concept of dose painting by contours (DPBC). However, our methodology lends itself to dose painting by numbers (DPBN) techniques, each voxel with low TCP values can be assigned to a corresponding escalated dose, leading to better matching of the escalated dose distribution to the high risk voxels for further TCP increase. To the best of our knowledge, there are no commercial treatment planning systems (TPS) facilitating the planning of DPBN. We will study this in the future.

Since some early-stage trials showed promising outcomes using proton therapy for GBM patients compared with photon therapy,[63–65] it is expected that proton therapy has the potential to widen the therapeutic window and can be considered for dose painting. In the future, we will investigate the potential to further increase TCP values by applying our proposed method using proton beam therapy (PBT), since PBT, which may offer more headroom for SIB dose-escalation due to the decrease in integral dose outside the target.

CONCLUSION

This study used ADC-driven SIB dose painting to escalate the dose to a certain area in the GTV for GBM patients. The results showed that TCP increases can be achieved without exceeding the baseline OAR tolerances. Patients with higher number of tumor cells, in other words, lower TCP, showed a higher potential for TCP increase with this methodology. In addition, ADC has been demonstrated as an imaging biomarker with a higher cell density for the selection of patients and is able to guide the escalation of the dose in a personalized way.

ACKNOWLEDGMENT

The authors wish to thank Dr Jailan Alshaikhi (University College London & University College London Hospital) for his help with the radiotherapy plan.

CONFLICTS OF INTEREST

The authors declare no conflict of interest with respect to the research, authorship, and/or publication of this article.

FUNDING

Author Yaru Pang was funded by China Scholarship Council.

REFERENCES

1. Schuster J, Lai RK, Recht LD, Reardon DA, Paleologos NA, Groves MD, et al. A phase II, multicenter trial of rindopepimut (CDX-110) in newly diagnosed glioblastoma: the act III study. *Neuro-Oncology* 2015; **17**: 854–61. https://doi.org/10.1093/neuonc/nou348
2. Stupp R, Mason WP, van den Bent MJ, Weller M, Fisher B, Taphoorn MJB, et al. Radiotherapy plus concomitant and adjuvant temozolomide for glioblastoma. *N Engl J Med* 2005; **352**: 987–96. https://doi.org/10.1056/NEJMoa043330

3. Weathers SP, Gilbert MR. Current challenges in designing GBM trials for immunotherapy. *J Neurooncol* 2015; **123**: 331–37. https://doi.org/10.1007/s11060-015-1716-2
4. Gilbert MR, Wang M, Aldape KD, Stupp R, Hegi ME, Jaeckle KA, et al. Dose-Dense temozolomide for newly diagnosed glioblastoma: A randomized phase III clinical trial. *JCO* 2013; **31**: 4085–91. https://doi.org/10.1200/JCO.2013.49.6968
5. Kirkpatrick JP, Laack NN, Shih HA, Gondi V. Management of GBM: A problem of local recurrence. *J Neurooncol* 2017; **134**: 487–93. https://doi.org/10.1007/s11060-016-2347-y
6. Gebhardt BJ, Dobelbower MC, Ennis WH, Bag AK, Markert JM, Fiveash JB. Patterns of failure for glioblastoma multiforme following limited-margin radiation and concurrent temozolomide. *Radiat Oncol* 2014; **9**: 130. https://doi.org/10.1186/1748-717X-9-130
7. Choi SH, Kim JW, Chang JS, Cho JH, Kim SH, Chang JH, et al. Impact of including peritumoral edema in radiotherapy target volume on patterns of failure in glioblastoma following temozolomide-based chemoradiotherapy. *Sci Rep* 2017; **7**: 42148. https://doi.org/10.1038/srep42148
8. Tini P, Nardone V, Pastina P, Battaglia G, Miracco C, Carbone SF, et al. Epidermal growth factor receptor expression predicts time and patterns of recurrence in patients with glioblastoma after radiotherapy and temozolomide. *World Neurosurg* 2018; **109**: e662–68. https://doi.org/10.1016/j.wneu.2017.10.052
9. Gromeier M, Brown MC, Zhang G, Lin X, Chen Y, Wei Z, et al. Very low mutation burden is a feature of inflamed recurrent glioblastomas responsive to cancer immunotherapy. *Nat Commun* 2021; **12**: 352. https://doi.org/10.1038/s41467-020-20469-6
10. Nakagawa K, Aoki Y, Fujimaki T, Tago M, Terahara A, Karasawa K, et al. High-Dose conformal radiotherapy influenced the pattern of failure but did not improve survival in glioblastoma multiforme. *Int J Radiat Oncol Biol Phys* 1998; **40**: 1141–49. https://doi.org/10.1016/s0360-3016(97)00911-5
11. Fitzek MM, Thornton AF, Rabinov JD, Lev MH, Pardo FS, Munzenrider JE, et al. Accelerated fractionated proton/photon irradiation to 90 cobalt gray equivalent for glioblastoma multiforme: Results of a phase II prospective trial. *J Neurosurg* 1999; **91**: 251–60. https://doi.org/10.3171/jns.1999.91.2.0251
12. Ling CC, Humm J, Larson S, Amols H, Fuks Z, Leibel S, et al. Towards multidimensional radiotherapy (MD-CRT): Biological imaging and biological conformality. *Int J Radiat Oncol Biol Phys* 2000; **47**: 551–60. https://doi.org/10.1016/s0360-3016(00)00467-3
13. ClinicalTraials.gov. NCT01504815. Adaptive radiation treatment for head and neck cancer (ARTFORCE). Available from: https://clinicaltrials.gov/ct2/show/NCT01504815
14. Madani I, Duthoy W, Derie C, De Gersem W, Boterberg T, Saerens M, et al. Positron emission tomography-guided, focal-dose escalation using intensity-modulated radiotherapy for head and neck cancer. *Int J Radiat Oncol Biol Phys* 2007; **68**: 126–35. https://doi.org/10.1016/j.ijrobp.2006.12.070
15. Madani I, Duprez F, Boterberg T, Van de Wiele C, Bonte K, Deron P, et al. Maximum tolerated dose in a phase I trial on adaptive dose painting by numbers for head and neck cancer. *Radiother Oncol* 2011; **101**: 351–55. https://doi.org/10.1016/j.radonc.2011.06.020
16. Berwouts D, Olteanu LAM, Duprez F, Vercauteren T, De Gersem W, De Neve W, et al. Three-phase adaptive dose-painting-by-numbers for head-and-neck cancer: Initial results of the phase I clinical trial. *Radiother Oncol* 2013; **107**: 310–16. https://doi.org/10.1016/j.radonc.2013.04.002
17. Buizza G, Molinelli S, D'Ippolito E, Fontana G, Pella A, Valvo F, et al. MRI-based tumour control probability in skull-base chordomas treated with carbon-ion therapy. *Radiother Oncol* 2019; **137**: 32–37. https://doi.org/10.1016/j.radonc.2019.04.018
18. Grönlund E, Johansson S, Nyholm T, Thellenberg C, Ahnesjö A. Dose painting of prostate cancer based on Gleason score correlations with apparent diffusion coefficients. *Acta Oncol* 2018; **57**: 574–81. https://doi.org/10.1080/0284186X.2017.1415457
19. Douglas JG, Stelzer KJ, Mankoff DA, Tralins KS, Krohn KA, Muzi M, et al. [F-18] -fluorodeoxyglucose positron emission tomography for targeting radiation dose escalation for patients with glioblastoma multiforme: Clinical outcomes and patterns of failure. *Int J Radiat Oncol Biol Phys* 2006; **64**: 886–91. https://doi.org/10.1016/j.ijrobp.2005.08.013
20. Piroth MD, Pinkawa M, Holy R, Klotz J, Schaar S, Stoffels G, et al. Integrated boost IMRT with FET-PET-adapted local dose escalation in glioblastomas. *Strahlenther Onkol* 2012; **188**: 334–39. https://doi.org/10.1007/s00066-011-0060-5
21. Tsien CI, Brown D, Normolle D, et al. Concurrent temozolomide and dose-escalated intensity-modulated radiation therapy in newly diagnosed glioblastomaradiation dose escalation and concurrent temozolomide in primary GB[J]. *Clin Cancer Res* 2012; **18**: 273–79.
22. Ken S, Vieillevigne L, Franceries X, Simon L, Supper C, Lotterie J-A, et al. Integration method of 3D MR spectroscopy into treatment planning system for glioblastoma IMRT dose painting with integrated simultaneous boost. *Radiat Oncol* 2013; **8**: 1–9. https://doi.org/10.1186/1748-717X-8-1
23. Laprie A, Ken S, Filleron T, Lubrano V, Vieillevigne L, Tensaouti F, et al. Dose-painting multicenter phase III trial in newly diagnosed glioblastoma: The SPECTRO-GLIO trial comparing arm a standard radiochemotherapy to arm B radiochemotherapy with simultaneous integrated boost guided by mr spectroscopic imaging. *BMC Cancer* 2019; **19**(1): 167. https://doi.org/10.1186/s12885-019-5317-x
24. Kosztyla R, Raman S, Moiseenko V, Reinsberg SA, Toyota B, Nichol A. Dose-painted volumetric modulated Arc therapy of high-grade glioma using 3,4-dihydroxy-6-[18F] fluoro-l-phenylalanine positron emission tomography. *Br J Radiol* 2019; **92**(1099): 20180901. https://doi.org/10.1259/bjr.20180901
25. Lindvall O, Kokaia Z. Stem cells for the treatment of neurological disorders. *Nature* 2006; **441**: 1094–96. https://doi.org/10.1038/nature04960
26. Eyler CE, Rich JN. Survival of the fittest: Cancer stem cells in therapeutic resistance and angiogenesis. *J Clin Oncol* 2008; **26**: 2839–45. https://doi.org/10.1200/JCO.2007.15.1829
27. Gallaher JA, Massey SC, Hawkins-Daarud A, Noticewala SS, Rockne RC, Johnston SK, et al. From cells to tissue: How cell scale heterogeneity impacts glioblastoma growth and treatment response. *PLoS Comput Biol* 2020; **16**(2): e1007672. https://doi.org/10.1371/journal.pcbi.1007672
28. Ahmad S, Prescott KB, Vlachaki MT. Surviving fraction (SF2) and clonogen cell density (ccd) are the dominant predictors of tumor control probability (TCP) in high grade glioma. *International Journal of Radiation Oncology*Biology*Physics* 2007; **69**: S692. https://doi.org/10.1016/j.ijrobp.2007.07.2062
29. Doskaliyev A, Yamasaki F, Ohtaki M, Kajiwara Y, Takeshima Y, Watanabe Y, et al. Lymphomas and glioblastomas: Differences in the apparent diffusion coefficient evaluated with high b-value diffusion-weighted magnetic resonance imaging at 3T. *Eur J Radiol* 2012; **81**: 339–44. https://doi.org/10.1016/j.ejrad.2010.11.005
30. Ellingson BM, Malkin MG, Rand SD, Connelly JM, Quinsey C, LaViolette PS, et al. Validation of functional diffusion maps (fdms) as a biomarker for human glioma

cellularity. *J Magn Reson Imaging* 2010; **31**: 538–48. https://doi.org/10.1002/jmri.22068
31. Dewey WC, Hopwood LE, Sapareto SA, Gerweck LE. Cellular responses to combinations of hyperthermia and radiation. *Radiology* 1977; **123**: 463–74. https://doi.org/10.1148/123.2.463
32. Stamatakos GS, Antipas VP, Uzunoglu NK, Dale RG. A four-dimensional computer simulation model of the in vivo response to radiotherapy of glioblastoma multiforme: Studies on the effect of clonogenic cell density. *Br J Radiol* 2006; **79**: 389–400. https://doi.org/10.1259/bjr/30604050
33. Kikuchi T, Kumabe T, Higano S, Watanabe M, Tominaga T. Minimum apparent diffusion coefficient for the differential diagnosis of ganglioglioma. *Neurol Res* 2009; **31**: 1102–7. https://doi.org/10.1179/174313209X382539
34. Murakami R, Hirai T, Kitajima M, Fukuoka H, Toya R, Nakamura H, et al. Magnetic resonance imaging of pilocytic astrocytomas: Usefulness of the minimum apparent diffusion coefficient (ADC) value for differentiation from high-grade gliomas. *Acta Radiol* 2008; **49**: 462–67. https://doi.org/10.1080/02841850801918555
35. Hayashida Y, Hirai T, Morishita S, Kitajima M, Murakami R, Korogi Y, et al. Diffusion-weighted imaging of metastatic brain tumors: Comparison with histologic type and tumor cellularity. *AJNR Am J Neuroradiol* 2006; **27**: 1419–25.
36. Chen J, Xia J, Zhou Y, Xia L, Zhu W, Zou M, et al. Correlation between magnetic resonance diffusion weighted imaging and cell density in astrocytoma. *Zhonghua Zhong Liu Za Zhi* 2005; **27**: 309–11.
37. Guo AC, Cummings TJ, Dash RC, Provenzale JM. Lymphomas and high-grade astrocytomas: Comparison of water diffusibility and histologic characteristics. *Radiology* 2002; **224**: 177–83. https://doi.org/10.1148/radiol.2241010637
38. Kono K, Inoue Y, Nakayama K, Shakudo M, Morino M, Ohata K, et al. The role of diffusion-weighted imaging in patients with brain tumors. *AJNR Am J Neuroradiol* 2001; **22**: 1081–88.
39. Gauvain KM, McKinstry RC, Mukherjee P, Perry A, Neil JJ, Kaufman BA, et al. Evaluating pediatric brain tumor cellularity with diffusion-tensor imaging. *AJR Am J Roentgenol* 2001; **177**: 449–54. https://doi.org/10.2214/ajr.177.2.1770449
40. Gupta RK, Cloughesy TF, Sinha U, Garakian J, Lazareff J, Rubino G, et al. Relationships between choline magnetic resonance spectroscopy, apparent diffusion coefficient and quantitative histopathology in human glioma. *J Neurooncol* 2000; **50**: 215–26. https://doi.org/10.1023/a:1006431120031
41. Sugahara T, Korogi Y, Kochi M, Ikushima I, Shigematu Y, Hirai T, et al. Usefulness of diffusion-weighted MRI with echo-planar technique in the evaluation of cellularity in gliomas. *J Magn Reson Imaging* 1999; **9**: 53–60. https://doi.org/10.1002/(sici)1522-2586(199901)9:1<53::aid-jmri7>3.0.co;2-2
42. Eidel O, Neumann J-O, Burth S, Kieslich PJ, Jungk C, Sahm F, et al. Automatic analysis of cellularity in glioblastoma and correlation with ADC using trajectory analysis and automatic nuclei counting. *PLoS One* 2016; **11**(7): e0160250. https://doi.org/10.1371/journal.pone.0160250
43. Kim BS, Kim ST, Kim JH, Seol HJ, Nam DH, Shin HJ, et al. Apparent diffusion coefficient as a predictive biomarker for survival in patients with treatment-naive glioblastoma using quantitative multiparametric magnetic resonance profiling. *World Neurosurgery* 2019; **122**: e812–20. https://doi.org/10.1016/j.wneu.2018.10.151
44. Brancato V, Nuzzo S, Tramontano L, Condorelli G, Salvatore M, Cavaliere C. Predicting survival in glioblastoma patients using diffusion MR imaging metrics-A systematic review. *Cancers (Basel)* 2020; **12**(10): 2858. https://doi.org/10.3390/cancers12102858
45. Pedicini P, Fiorentino A, Simeon V, Tini P, Chiumento C, Pirtoli L, et al. Clinical radiobiology of glioblastoma multiforme. *Strahlenther Onkol* 2014; **190**: 925–32. https://doi.org/10.1007/s00066-014-0638-9
46. Center for Medical Imaging Computing. NiftyReg. Available from: http://cmictig.cs.ucl.ac.uk/wiki/index.php/NiftyReg
47. Ali S, Joseph NM, Perry A, Barajas RF, Cha S. Apparent diffusion coefficient in glioblastoma with PNET-like components, a GBM variant. *J Neurooncol* 2014; **119**: 353–60. https://doi.org/10.1007/s11060-014-1485-3
48. Barajas RF Jr, Hodgson JG, Chang JS, Vandenberg SR, Yeh R-F, Parsa AT, et al. Glioblastoma multiforme regional genetic and cellular expression patterns: Influence on anatomic and physiologic MR imaging. *Radiology* 2010; **254**: 564–76. https://doi.org/10.1148/radiol.09090663
49. Neska-Matuszewska M, Bladowska J, Sąsiadek M, Zimny A. Differentiation of glioblastoma multiforme, metastases and primary central nervous system lymphomas using multiparametric perfusion and diffusion MR imaging of a tumor core and a peritumoral zone-searching for a practical approach. *PLoS One* 2018; **13**(1): e0191341. https://doi.org/10.1371/journal.pone.0191341
50. Ko CC, Tai MH, Li CF, Chen TY, Chen JH, Shu G, et al. Differentiation between glioblastoma multiforme and primary cerebral lymphoma: Additional benefits of quantitative diffusion-weighted MR imaging. *PLoS One* 2016; **11**(9): e0162565. https://doi.org/10.1371/journal.pone.0162565
51. Bentzen SM, Gregoire V. Molecular imaging-based dose painting: A novel paradigm for radiation therapy prescription. *Semin Radiat Oncol* 2011; **21**: 101–10. https://doi.org/10.1016/j.semradonc.2010.10.001
52. Bentzen SM, Constine LS, Deasy JO, Eisbruch A, Jackson A, Marks LB, et al. Quantitative analyses of normal tissue effects in the clinic (QUANTEC): An introduction to the scientific issues. *Int J Radiat Oncol Biol Phys* 2010; **76**: S3–9. https://doi.org/10.1016/j.ijrobp.2009.09.040
53. Emami B, Lyman J, Brown A, Coia L, Goitein M, Munzenrider JE, et al. Tolerance of normal tissue to therapeutic irradiation. *Int J Radiat Oncol Biol Phys* 1991; **21**: 109–22. https://doi.org/10.1016/0360-3016(91)90171-y
54. Korreman SS, Ulrich S, Bowen S, Deveau M, Bentzen SM, Jeraj R. Feasibility of dose painting using volumetric modulated Arc optimization and delivery. *Acta Oncol* 2010; **49**: 964–71. https://doi.org/10.3109/0284186X.2010.498440
55. Bentzen SM. Theragnostic imaging for radiation oncology: Dose-painting by numbers. *Lancet Oncol* 2005; **6**: 112–17. https://doi.org/10.1016/S1470-2045(05)01737-7
56. Grönlund E, Johansson S, Montelius A, Ahnesjö A. Dose painting by numbers based on retrospectively determined recurrence probabilities. *Radiother Oncol* 2017; **122**: 236–41. https://doi.org/10.1016/j.radonc.2016.09.007
57. Orlandi M, Botti A, Sghedoni R, Cagni E, Ciammella P, Iotti C, et al. Feasibility of voxel-based dose painting for recurrent glioblastoma guided by ADC values of diffusion-weighted MR imaging. *Phys Med* 2016; **32**: 1651–58. https://doi.org/10.1016/j.ejmp.2016.11.106
58. Brenner DJ, Hlatky LR, Hahnfeldt PJ, Hall EJ, Sachs RK. A convenient extension of the linear-quadratic model to include redistribution and reoxygenation. *Int J Radiat Oncol Biol Phys* 1995; **32**: 379–90. https://doi.org/10.1016/0360-3016(95)00544-9
59. Laprie A, Noel G, Chaltiel L, Truc G, Sunyach M, Charissoux M, et al. OC-0333 dose-painting multicenter phase III trial in newly diagnosed glioblastoma: The SPECTRO-GLIO trial. *Radiotherapy and Oncology* 2021; **161**: S246–47. https://doi.org/10.1016/S0167-8140(21)06866-3

60. Singh R, Lehrer EJ, Wang M, Perlow HK, Zaorsky NG, Trifiletti DM, et al. Dose escalated radiation therapy for glioblastoma multiforme: An international systematic review and meta-analysis of 22 prospective trials. *Int J Radiat Oncol Biol Phys* 2021; **111**: 371–84. https://doi.org/10.1016/j.ijrobp.2021.05.001
61. Iuchi T, Hatano K, Kodama T, Sakaida T, Yokoi S, Kawasaki K, et al. Phase 2 trial of hypofractionated high-dose intensity modulated radiation therapy with concurrent and adjuvant temozolomide for newly diagnosed glioblastoma. *Int J Radiat Oncol Biol Phys* 2014; **88**: 793–800. https://doi.org/10.1016/j.ijrobp.2013.12.011
62. Stupp R, Hegi ME, Mason WP, van den Bent MJ, Taphoorn MJB, Janzer RC, et al. Effects of radiotherapy with concomitant and adjuvant temozolomide versus radiotherapy alone on survival in glioblastoma in a randomised phase III study: 5-year analysis of the EORTC-NCIC trial. *Lancet Oncol* 2009; **10**: 459–66. https://doi.org/10.1016/S1470-2045(09)70025-7
63. Liu EK, Sulman EP, Wen PY, Kurz SC. Novel therapies for glioblastoma. *Curr Neurol Neurosci Rep* 2020; **20**: 1–12. https://doi.org/10.1007/s11910-020-01042-6
64. Brown PD, Chung C, Liu DD, McAvoy S, Grosshans D, Al Feghali K, et al. A prospective phase II randomized trial of proton radiotherapy vs intensity-modulated radiotherapy for patients with newly diagnosed glioblastoma. *Neuro Oncol* 2021; **23**: 1337–47. https://doi.org/10.1093/neuonc/noab040
65. Mohan R, Liu AY, Brown PD, Mahajan A, Dinh J, Chung C, et al. Proton therapy reduces the likelihood of high-grade radiation-induced lymphopenia in glioblastoma patients: Phase II randomized study of protons vs photons. *Neuro Oncol* 2021; **23**: 284–94. https://doi.org/10.1093/neuonc/noaa182